Study of excitonic excited states in heterostructures with $MoSe_2$ monolayers

© G.M. Golyshkov, A.S. Brichkin, A.V. Chernenko

Osipyan Institute of Solid State Physics, Russian Academy of Sciences,
142432 Chernogolovka, Russia

E-mail: golyshkov.gm@phystech.edu

Received April 26, 2024
Revised April 27, 2024
Accepted April 27, 2024

Heterostructures based on $MoSe_2$ monolayers were studied using the method of optical reflection spectroscopy, and the excited states of excitons were studied. It is shown that the shape of the reflection spectrum of the ground and excited states is determined by the thickness of the hexagonal boron nitride used in the heterostructure. Numerical modeling using the calculation of the reflectance of a heterostructure via the transfer matrix method gives a good agreement between the experimental line shape and the theoretical one, which confirms the universality of this method and makes it convenient for further research of van der Waals structures with other materials and parameters.

Keywords: exciton, heterostructure, monolayer.

DOI: 10.61011/SC.2024.05.59168.6339H

1. Introduction

The monolayers of transition metals dichalcogenides (TMD) — are the direct-band-gap semiconductors with unique properties due to the band structure specifics and having such a band gap width that contributes to powerful light absorption in the visible spectral range. Powerful optical absorption is caused by excitons (correlated electron-hole pairs). Due to the low effective dielectric permittivity and large effective mass, the exciton bond energy reaches several hundreds meV, which makes it possible to observe exciton effects at temperatures up to room temperature [1]. This makes TMD monolayers promising objects both from the point of view of fundamental research and in terms of implementation of associated optoelectronic devices.

Encapsulation of TMD monolayers with hexagonal boron nitride (*h*BN) is a generally common in fabrication of such structures, since it leads to a significant narrowing of exciton lines due to a decrease in inhomogeneous broadening associated with the substrate, and in addition, such structures turn out to be much more resistant to the environment and repeated thermal cycling.

Various TMD structures with encapsulated monolayers have been studied in both, photoluminescence and reflection spectra. Apart from the main exciton resonance of A-exciton, a line of the B-exciton split off from the A-exciton through spin-orbital interaction in the valence band is also observed in the reflection spectrum [1]. Of great interest to researchers are excited exciton states, which are observed in the reflection spectra and allow estimating the bond energy of the exciton. In many studies the excited states are murky and they cane be qualitatively identified more often not in the initial spectrum, but only by means of averaging, smoothing and in 1-st derivative spectrum [4]. This paper outlines the findings of studying the exciton resonances in the reflection spectra of *h*BN-ML $MoSe_2$-*h*BN structures with a step-like bottom layer *h*BN. Due to high quality of these structures in the initial spectra the lines of A- and B-exciton, as well as excited states of A-exciton are clearly observed.

2. Experimental method

The studied heterostructures *h*BN-ML $MoSe_2$-*h*BN, fabricated by method of mechanical exfoliation, represent themselves the encapsulated monolayers $MoSe_2$, placed on the substrate SiO_2/Si 285 nm. According to method described in [2], the bottom layer *h*BN is placed on the substrate first, after that monolayer $MoSe_2$ is placed which is further covered with upper layer *h*BN. The main specifics of the studied structures is that the bottom layer was deliberately taken as a „step-like“ structure (see Figure 1), i.e. thickness of bottom layer *h*BN was controllably varied within the range of thicknesses from 20 to 260 nm. The upper layer *h*BN was taken homogeneous and relatively thin (7−10 nm) for all samples. Thus, it appeared that a slew of structures of various thickness*h*BN was assembled in similar conditions to minimize uncontrollable effects on the assembly process. Figure 1, *b* illustrates a photo of sample with denoted layers, where different color „steps“ A, B, C, D, are clearly observed corresponding, respectively, to different thickness of the bottom layer *h*BN.

Thickness of layers *h*BN was defined by profilometer and atomic-force microscope (AFM). Measurements were made in helium filling cryostat for optical measurements with temperature stabilization system in the range of 2−295 K. The reflection spectra were measured using a halogen

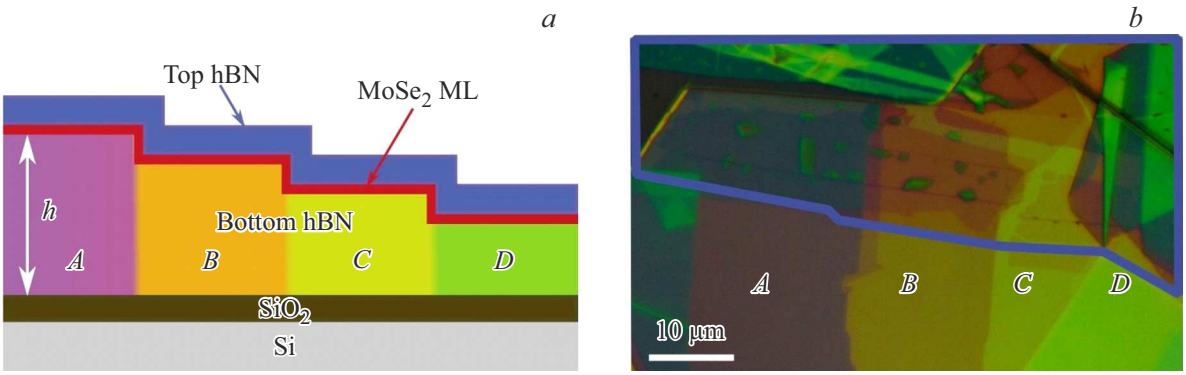

Figure 1. *a* — scheme of heterostructure *h*BN-$MoSe_2$-*h*BN with thickness gradient (with a step-like structure) of the bottom layer *h*BN. *b* — photo of a step-like structure sample on SiO_2/Si substrate with silicon oxide 285 nm thick. Blue line defines the boundary of upper *h*BN layer. Areas of sample with different thickness of bottom layer *h*BN are distinctly separated by colors. On photo the denoted areas of bottom *h*BN layer have the following thicknesses, nm: *A* — 130, *B* — 115, *C* — 100, *D* — 90. (A color version of the figure is provided in the online version of the paper).

lamp, the light from which was passed through a crossed slit and focused on the surface of the structure through Mitutoyo lens ($\times 50$) into a spot with a size of $2-3\,\mu$m. The reflection signal was focused on the input slit of the monochromator and detected by a cooled charge-coupled device (CCD camera). Position of the reflection lines of the ground and excited exciton states in the spectrum can vary significantly depending on the sample position. This occurs because of the structure inhomogeneities, first of all because of formation of „bubbles“ on the interfaces [2,6], therefore, for each „step“ (area of the sample with thickness homogeneous bottom layer *h*BN) one position on the sample was selected optimal in terms of signal intensity, line width. The required condition for the observation of excited states was a „fine“ focusing of the light beam (in spot no more than $3\,\mu$m in size). The appropriate „background“ signal was recorded for each spectra for the selected point on the sample from the monolayer-free position with the same thicknesses of layers *h*BN (see insert in Figure 2). The temperature stabilization system and presence of precision piezoelectric movements make it possible to control the position on the sample with an accuracy of $1\,\mu$m and observe excited states in the temperature range $2-110$ K.

3. Experimental findings and discussion

The lines of exciton resonances have good resolution in the reflection spectra as shown in Figures 2–4. For most of the structures in spectra at helium temperatures an intensive line is observed corresponding to the ground exciton state A:1*s* with energy of ~ 1.64 eV. Also in the spectra we may see transitions with much higher energies related to excited exciton states [8]. The line with energy of ~ 1.85 eV corresponds to the ground B-exciton state (B:1*s*). Other lines are related to the excited states of A-exciton (A:2*s* and A:3*s*). Splitting between A:2*s*–A:1*s* and A:3*s*–A:2*s* makes 150 ± 1 meV and 34 ± 1 meV, respectively. With the temperature growth, the resonances become wider and shift towards lower energies (Figure 3). At temperature of 77 K it is impossible to resolve A:3*s* against wide B:1*s*, however, splitting of up to 110 K A:2*s*–A:1*s* remains the same as with low temperature. From this it follows that the exciton bond energy changes slightly with the growth of temperature, and the main contribution to the shift of the exciton line is determined by a temperature decrease in the band gap [2].

For positions on a sample with different thicknesses of the bottom layer *h*BN, a significant variation in the shape of exciton resonances in spectra is observed. Figure 4 shows that for position № 1 (160 nm) exciton resonances are manifested by more than an order more distinctly, compared to position № 2 (122 nm), and with variation of thickness from position № 2 (122 nm) to position № 3 (100 nm) the shape of line A:2*s* changes from a „dip“ to „peak“. The shape of line of B-exciton ground state also significantly changes. This is because the reflection spectrum from the layered van der Waals structure is formed not only by the TMD monolayer itself, but also by the layers *h*BN and the permeability substrate.

Analysis of the differential reflectance shown in Figure 2 and 4, were performed by numerical modeling of the layered structure reflectance using formalism of the transfer matrix method [3,7]. At normal light incidence, the transfer matrices of the individual layers of the structure look as follows:

for homogeneous layers —

$$\hat{T}_{\text{hom}} = \begin{pmatrix} e^{ikL} & 0 \\ 0 & e^{-ikL} \end{pmatrix}, \qquad (1)$$

$k = \frac{\omega n}{c}$ — wave number, n — refractive index, L — layer thickness;

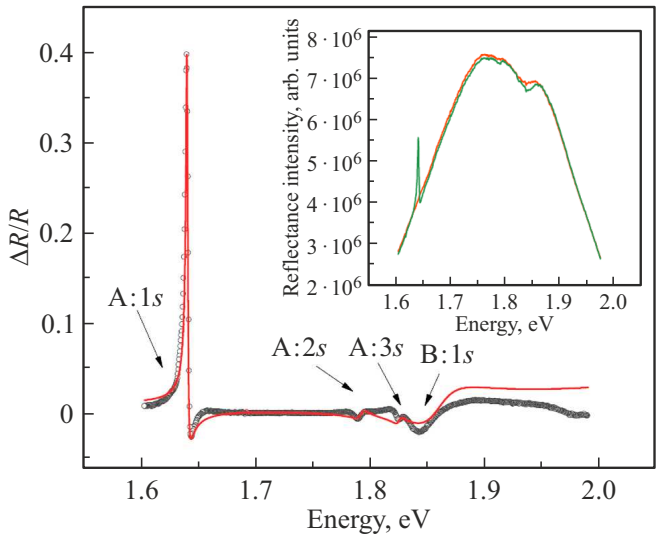

Figure 2. Differential reflectance$\Delta R/R_{\text{sub}}$ for encapsulated monolayers $MoSe_2$. The points designate experimental results obtained at $T = 2$ K. Low-energy peak corresponds to the ground exciton resonance A:1s. Singularities with higher energies are related to the first two excited states of A-exciton (A:2s and A:3s) and ground state of B-exciton. Red line denotes the differential reflectance numerically modelled with the use of layers thicknesses (thickness of upper layer hBN — 10 nm, thickness of lower layer hBN — 130 nm, thickness of SiO_2 — 285 nm), close to the values defined with the use of AFM. Parameters of exciton resonances $\gamma_{\text{A:1s}} = 3$ meV, $\gamma_{0,\text{A:1s}} = 0.7$ meV, $\gamma_{0,\text{A:2s}} = 0.06$ meV, $\gamma_{0,\text{A:3s}} = 0.03$ meV, $\gamma_{\text{B:1s}} = 0.9$ meV, $\gamma_{0,\text{B:1s}} = 22$ meV. The insert shows the sample reflection spectra for position with monolayer (green line) and without monolayer (orange line). Refractive indices $n_{h\text{BN}} = 2.2$; $n_{SiO_2} = 1.46$ and $n_{\text{Si}} = 3.5$.

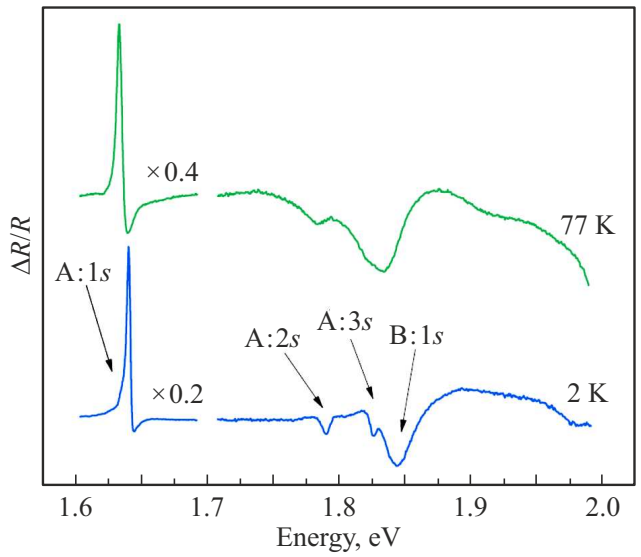

Figure 3. Differential reflectance for heterostructure with monolayer $MoSe_2$, recorded at two different temperatures $T = 2$ K (blue color) and 77 K (green color). Ground state A:1s multiplied by appropriate coefficients.

for interlayer boundary —

$$\hat{T}_{n_1 \to n_2} = \frac{1}{2n_1} \begin{pmatrix} n_1 + n_2 & n_2 - n_1 \\ n_2 - n_1 & n_2 + n_1 \end{pmatrix} \tag{2}$$

when light is passing from the layer with refractive index n_1 into the layer with refractive index n_2;

for TMD monolayer —

$$\hat{T}_{\text{TMD}} = \frac{1}{t} \begin{pmatrix} t^2 - r^2 & r \\ -r & 1 \end{pmatrix}, \tag{3}$$

where t and r — absorption coefficient and reflectance, $t = 1 + r$. The amplitude reflectance of TMD monolayers includes individual contributions of A- and B-excitons series, which are well separated.

$$r(\hbar\omega) = \sum_{j=1}^{3} \frac{i \cdot \gamma_{0,\text{A:}js}}{\hbar\omega_{\text{A:}js} - \hbar\omega - i \cdot (\gamma_{0,\text{A:}js} + \gamma_{\text{A}})} + \frac{i \cdot \gamma_{0,\text{B:1s}}}{\hbar\omega_{\text{B:1s}} - \hbar\omega - i \cdot (\gamma_{0,\text{B:1s}} + \gamma_{\text{B}})}, \tag{4}$$

$\omega_{\text{A:}js}$ and $\omega_{\text{B:1s}}$ — resonance frequencies, γ_0 andγ — radiation-induced and non-radiative decay of excitons.

The transfer matrix for a heterostructure with a TMD monolayer is written as

$$\hat{T}_{\text{tot}} = \begin{pmatrix} T_{11} & T_{12} \\ T_{21} & T_{22} \end{pmatrix} = \hat{T}_{SiO_2 \to \text{Si}} \cdot \hat{T}_{SiO_2} \cdot \hat{T}_{h\text{BN} \to SiO_2} \times \hat{T}_{\text{bott } h\text{BN}} \cdot \hat{T}_{TMD} \cdot \hat{T}_{\text{top } h\text{BN}} \cdot \hat{T}_{\text{air} \to h\text{BN}}. \tag{5}$$

In paper [3] the final transfer matrix additionally includes matrices $\hat{T}_{\text{air} \to h\text{BN}}$ and $\hat{T}_{h\text{BN} \to \text{air}}$ around the monolayer. However, these factors do not significantly affect the reflectance. It is also assumed that the thickness of the Si layer is greater than the absorption depth, so the reflection at the boundary of Si and air is not taken into account. The reflectance from a heterostructure is determined as

$$R_{\text{tot}} = \left| \frac{T_{21}}{T_{22}} \right|^2. \tag{6}$$

To calculate the differential reflectance, it is required to calculate the reflectance from a structure without a monolayer R_{sub}. The transfer matrix in this case is written as

$$\hat{T}_{\text{tot}} = \hat{T}_{SiO_2 \to \text{Si}} \cdot \hat{T}_{SiO_2} \cdot \hat{T}_{h\text{BN} \to SiO_2} \cdot \hat{T}_{\text{bott } h\text{BN}} \cdot \hat{T}_{\text{top } h\text{BN}} \cdot \hat{T}_{\text{air} \to h\text{BN}}. \tag{7}$$

The reflectance for a monolayer-free structure is calculated similarly (6). The resultant differential reflectance is written as

$$\frac{\Delta R}{R} = \frac{R_{\text{tot}} - R_{\text{sub}}}{R_{\text{sub}}}. \tag{8}$$

In calculations the radiation-induced and non-radiative decays of the ground and excited states of excitons $\gamma_{0\text{A:}is}$, γ_{A},

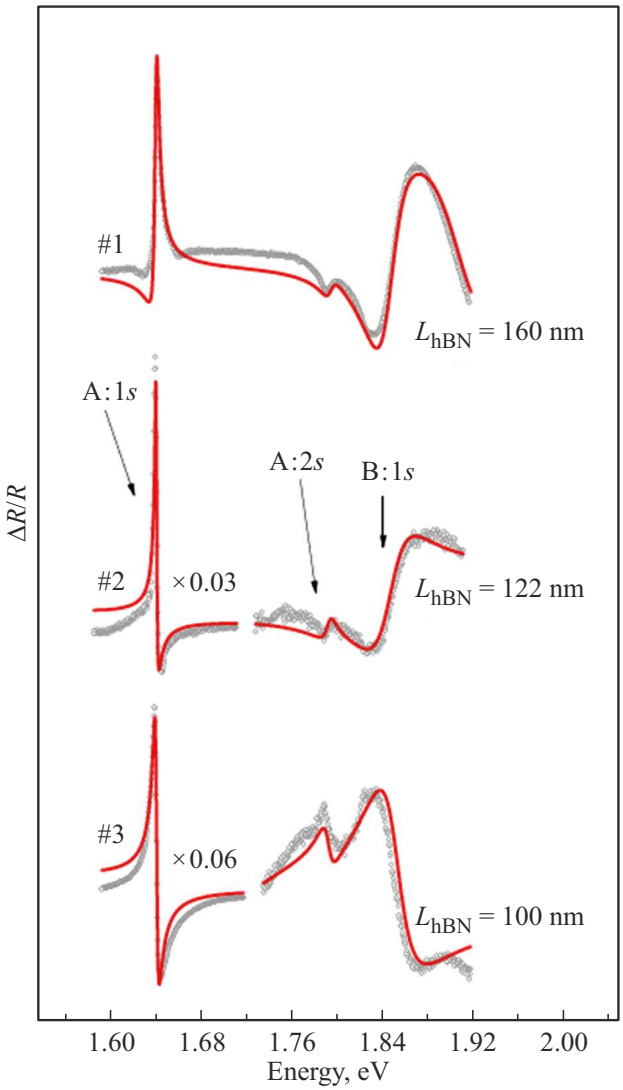

Figure 4. Differential reflectance of encapsulated monolayers $MoSe_2$, which have different thickness of bottom layer *h*BN. Conditions 1*s*, 2*s* of A-exciton and 1*s* B-exciton are indicated by arrows. Red lines — results of approximation of spectrum obtained by means of model described in the text. Thickness of layer SiO_2 — 285 nm, thickness of upper layer*h*BN — 7 nm, thickness of bottom layer *h*BN was an adjustable parameter along with parameter γ characterizing the reflection lines width. The thickness of layers *h*BN, found in this way, are illustrated in Figure for each spectrum.

γ_B were used as adjustable parameters, where $s = 1, 2, 3$, and defined the line of exciton resonance width in the differential reflectance; thickness of bottom layer *h*BN d_{hBN}, included in $\hat{T}_{hom}$, as well as energies of exciton resonances ω_{res}. Thickness of upper layer*h*BN was found using AFM and was taken equal 7–10 nm. Optimal shape of the approximation line was found by least-square method. The values of thickness of the bottom layer *h*BN found in this way turned out to be consistent with the values measured using AFM.

The results of numerical modeling describe well not only the shape of the ground state of A- and B-excitons (Figure 4), but also the shape of the excited states, which, with an increase in thickness from 100 nm to 122nm, changes from „peak“ to „dip“, which corresponds to the experimental results shown in Figure 4 for positions № 3 and 2, respectively. It should be expected that this model is quite versatile and will work well for other TMD materials, and other types and thicknesses of substrates.

The observed excited states are all indicative of high quality of the fabricated structures. This is also indicated by the line widths in the spectra approaching the radiation width [5].

4. Conclusion

Studies of the reflection spectra of structures containing monolayers $MoSe_2$ made it possible to observe the basic states of A- and B-excitons, in the initial reflection spectrum, as well as identify the reflection lines of 2*s*, 3*s* A-excitons. It is found that the bond energy of exciton excited states is practically independent of temperature in the range 2–110 K.

The reflection spectra of multilayer structures are well approximated using a model based on the transfer matrix method. The findings of theoretical modeling carried out for various thicknesses of *h*BN, showing how the depth and shape of exciton resonances depend on the thickness of individual layers [3], is confirmed experimentally in this study. It was demonstrated that selection of appropriate thicknesses of *h*BN and SiO_2 layers in structures fabrication allows obtaining the enhancement or inhibition of the exciton resonances. The study findings provide high potential for further investigation of the reflection spectra of TMD structures with the use of other materials and parameters.

Acknowledgments

Authors express their thanks to M. Glazov for inappreciable discussions of the treatment methods.

Conflict of interest

The authors declare that they have no conflict of interest.

References

[1] G. Wang, A. Chernikov, M. Glazov, T.F. Heinz, X. Marie, T. Amand, B. Urbaszek. Rev. Mod. Phys., **90**, 021001 (2018).
[2] A.S. Brichkin, G.M. Golyshkov, A.V. Chernenko. ZhETF **163**, 852 (2023). (in Russian).
[3] C. Robert, M.A. Semina, F. Cadiz, M. Manca, E. Courtade, T. Taniguchi, K. Watanabe, H. Cai, S. Tongay, B. Lassagne, P. Renucci, T. Amand, X. Marie, M.M. Glazov, B. Urbaszek. Phys. Rev. Mater., **2**, 0110 (2018).

[4] A. Chernikov, A.M. van der Zande., H.M. Hill, A.F. Rigosi, A. Velauthapillai, J. Hone, T.F. Heinz. Phys. Rev. Lett., **115**, 126802 (2015).
[5] G. Moody, D.C. Kavir, K. Hao, C.-H. Chen, L.-J. Li, A. Singh, K. Tran, G. Clark, X. Xu, G. Berghäuser, E. Malic, A. Knorr, X. Li. Nature Commun., **6**, 8315 (2015).
[6] A.V. Chernenko., A.S. Brichkin, G.M. Golyshkov, A.F. Shevchun Izv. RAN. Ser. Phys., **87**, 189 (2023). (in Russian).
[7] H.H. Fang, B. Han, C. Robert, M.A. Semina, D. Lagarde, E. Courtade, T. Taniguchi, K. Watanabe, T. Amand, B. Urbaszek, M.M. Glazov, X. Marie. Phys. Rev. Lett., **123**, 067401 (2019).
[8] B. Han, C. Robert, E. Courtade, M. Manca, S. Shree, T. Amand, P. Renucci, T. Taniguchi, K. Watanabe, X. Marie, L.E. Golub, M.M. Glazov, B. Urbaszek. Phys. Rev. X, **8**, 031073 (2018).

Translated by T.Zorina